Assessment of Myocardial Metabolism in Diabetic Rats Using Small-Animal PET: A Feasibility Study

Michael J. Welch, PhD; Jason S. Lewis, PhD; Joonyoung Kim, PhD; Terry L. Sharp, RT(R); Carmen S. Dence, MS; Robert J. Gropler, MD; and Pilar Herrero, MS

The Division of Radiological Sciences, Mallinckrodt Institute of Radiology, Washington University School of Medicine, St. Louis, Missouri

This feasibility study was undertaken to determine whether kinetic modeling in conjunction with small-animal PET could noninvasively quantify alterations in myocardial perfusion and substrate metabolism in rats. **Methods:** All small-animal PET was performed on either of 2 tomographs. Myocardial blood flow and substrate metabolism were measured in 10 male Zucker diabetic fatty rats (ZDF, *fa/fa*) and 10 lean littermates (Lean, *Fa/+*) using ^{15}O-water, 1-^{11}C-glucose, 1-^{11}C-acetate, and 1-^{11}C-palmitate. Animals were 12.0 ± 1.4-wk old. **Results:** Consistent with a type 2 diabetic phenotype, the ZDF animals showed higher plasma hemoglobin A_{1c}, insulin, glucose, and free fatty acid (FFA) levels than their lean controls. Myocardial glucose uptake (mL/g/min) was not significantly different between the 2 groups. However, higher glucose plasma levels in the ZDF rats resulted in higher myocardial glucose utilization (nmol/g/min) (Lean, 629 ± 785, vs. ZDF, 1,737 ± 1,406; $P = 0.06$). Similarly, myocardial FFA uptake (mL/g/min) was not significantly different between the 2 groups, (Lean, 0.51 ± 28, vs. ZDF, 0.72 ± 0.19; P = not significant) However, due to higher FFA plasma levels, utilization and oxidation (nmol/g/min) were significantly higher in the ZDF group (Lean, 519 ± 462, vs. ZDF, 1,623 ± 712, $P < .001$; and Lean, 453 ± 478, vs. ZDF, 1,636 ± 730, $P < .01$). **Conclusion:** Noninvasive measurements of myocardial substrate metabolism in ZDF rats using small-animal PET are consistent with the expected early metabolic abnormalities that occur in this well-characterized model of type 2 diabetes mellitus. Thus, small-animal PET demonstrates significant promise in providing a means to link the myocardial metabolic abnormalities that occur in rat of disease with the human condition.

Key Words: metabolism; diabetes mellitus; fatty acids; imaging; PET

J Nucl Med 2006; 47:689–697

Noninvasive imaging technologies have led to exceptional advances in the biomedical sciences in recent years. Most recently, many of the noninvasive imaging technologies that are used in humans have been miniaturized to permit imaging in small animals (*1*). The goal of these small-animal imaging devices is to obtain anatomic, physiologic, or biochemical information in small-animal models of disease that is the same as that obtained in humans and, thus, facilitate the correlation of research findings between bench and bedside. Moreover, the noninvasive capability of these imaging methods permits multiple acquisitions of this information, facilitating the assessment of temporal changes in disease or responses to new therapies in the same animal.

Results of studies in small animals are now showing that alterations in myocardial substrate metabolism plays a key role in variety of normal and abnormal cardiac states, such as normal aging, hypertension-induced left ventricular hypertrophy, obesity, and diabetic heart disease. For example, we have previously shown that it is possible to qualitatively show differences in cardiac metabolism in a transgenic model of diabetes in which PPARα (peroxisome proliferator-activated receptor α) is upregulated (*2*). Thus, the ability to quantify myocardial metabolism in both normal and diseased rodents will have direct ramifications on the development of potential therapies and their translation into clinical practice (*3*).

The advent of small-animal PET technology allows for the sequential measurements of cardiac metabolic rates in the same animal (*4–6*). This current feasibility study was aimed at validating the use of PET to address the general hypothesis that rat models of cardiac disease in conjunction with small-animal PET can be used to quantify alterations in myocardial substrate metabolism in the rat myocardium. In this study we used a rat model of type 2 diabetes mellitus (Zucker diabetic fatty [ZDF] rats) to examine the feasibility of using small-animal PET, and kinetic modeling techniques extensively validated in large animals (*7–11*) and currently used in humans (*12–16*), to detect noninvasively changes in myocardial substrate metabolism in vivo in rats.

MATERIALS AND METHODS

All chemicals, unless otherwise stated, were purchased from Aldrich Chemical Co., Inc. ^{15}O-Water (*17*), 1-^{11}C-glucose (*18*),

Received Sep. 19, 2005; revision accepted Nov. 16, 2005.

For correspondence contact: Pilar Herrero, MS, Mallinckrodt Institute of Radiology, Washington University School of Medicine, Campus Box 8225, 510 S. Kingshighway Blvd., St. Louis, MO 63110.

E-mail: herrerop@mir.wustl.edu

and 1-^{11}C-palmitate (*19*) were all synthesized according to published methods. 1-^{11}C-Acetate is produced routinely in our laboratory with a commercially available acetate module (CTI). Radioactive samples were counted on a Beckman 8000 γ-counter. Small-animal PET was performed on either the microPET R4 (*20*) or the microPET Focus (*21*) tomograph (Concorde Microsystems Inc.) housed in a temperature-controlled imaging suite.

Animal Preparation

All animal experiments were conducted in compliance with the Guidelines for the Care and Use of Research Animals established by Washington University's Animal Studies Committee. Optimal animal handling methods for small-animal PET have been extensively studied by our group and have been reported elsewhere (*22*). Ten male ZDF rats (*fa/fa*) and their corresponding matched lean littermates (Lean, *Fa/+*), from Charles River Laboratories, Inc. (Table 1), were fed Purina Constant Nutrition 5008, consisting of 26.8% protein, 16.7% fat, and 56.4% carbohydrates. Before the imaging studies, rats were placed in metabolism cages and were fasted from food for 6 h with water being given ad lib. On each study day the rats were anesthetized with 2%–2.5% isoflurane inhaled anesthesia via an induction chamber. Maintenance of anesthesia throughout the procedure consisted of 1%–1.5% isoflurane via a custom-designed nose cone. The rat's neck was shaved and scrubbed, in preparation for a sterile cutdown procedure. A 1- to 1.5-cm incision was made over the right jugular vein. The vein was exposed and ligated, and a microrenathane catheter (0.025-mm outer diameter × 0.012-mm inner diameter) was sutured in place. The rat was globally heparinized (10 mg/kg) to prevent the catheter from clotting. Body temperature was maintained using a circulating water blanket as well as a heat lamp. Pediatric electrocardiogram leads (Red Dot Infant Electrodes; M.M.M. Co.) were placed on the rat's hind limbs to measure and record heart rate.

Glucose/Acetate/Palmitate (GAP) Study Methods and Procedures

The animals were secured in a custom-designed acrylic restraining device, placed within the PET scanner with dynamic imaging acquisition starting 5 s after a bolus injection of tracer via the right jugular catheter. Littermates were scanned sequentially during the same scanning session. The GAP imaging protocol (*16*) consisted of dynamic acquisition of microPET images of ^{15}O-water (37 MBq), 1-^{11}C-acetate (11–15 MBq), 1-^{11}C-glucose (11–15 MBq), and 1-^{11}C-palmitate (11–15 MBq) radiotracers (Figs. 1 and 2). 1-^{11}C-Glucose is used to quantify glucose metabolism, rather than ^{18}F-FDG, because of the shorter radioactive half-life of ^{11}C, and this approach can quantify myocardial glucose utilization more accurately than ^{18}F-FDG PET (*7*). Total GAP PET sessions lasted 4–6 h. ^{15}O-Water data collection consisted of 5-s frames over 5 min (60 frames). For all of the metabolic tracers, each data collection consisted of 5 s × 24 frames, 15 s × 12 frames, 30 s × 10 frames, and 60 s × 10 frames (20 min total). Six whole-blood arterial samples were collected throughout the GAP study to measure whole blood glucose (5 μL), free fatty acid (FFA; 20 μL), and insulin (5 μL) levels. Heart and respiration rates were also recorded at baseline and throughout the study. To correct radioactivity in the blood (the input function needed for kinetic modeling) for the presence of ^{11}C-metabolites, a different set of blood samples was also taken during metabolic imaging.

Substrate Analysis

All substrate measurements were performed using commercially available, well-documented methods that have been validated in small animals (*22*). Briefly, whole blood (20–25 μL) was drawn into a Wiretrol II precision disposable micropipette (Drummond Scientific Co.) for insulin and FFA analysis. The blood was spun in a microcentrifuge (13,460*g* for 2 min) to separate red blood cells and plasma. The plasma was immediately placed in a −80°C freezer until analyzed. FFA levels were measured using a standard Nefa-C kit (Wako Chemicals USA, Inc.) by the Diabetes and Metabolism Core Laboratory of the Washington University School of Medicine (WUSM), Department of Endocrinology. Insulin levels were measured using a Rat Insulin ELISA Test kit (Crystal Chem, Inc.) by the Developmental Biology Core Laboratory of the WUSM, Department of Pediatrics. Plasma glucose levels were measured by placing whole blood (1 μL) on a glucose test strip for immediate analysis (using an Accu-Chek Plasma blood glucose analyzer [Roche Diagnostics, Inc.]).

Metabolite Measurements

During each metabolic imaging session, arterial whole blood samples were taken at 2, 5, 10, 15, and 20 min after each tracer

TABLE 1
Characteristics, Plasma Substrate Levels, and Hemodynamics of ZDF and Lean Rats Used in GAP Small-Animal PET Studies

Parameter	Lean (COV), $n = 10$	ZDF (COV), $n = 10$	Statistics (P, ZDF vs. Lean)
Age (wk)	12 ± 1.4	12 ± 1.4	NS
Weight (g)	283 ± 47	343 ± 57	<0.02
HbA_{1c}	3.09 ± 0.33	7.25 ± 1.48	<0.0001 (COV, NS)
Insulin (μU/mL)	23.08 ± 6.31 (27.2 ± 12.2)	57.04 ± 28.08 (22.4 ± 10.4)	<0.0001 (COV, NS)
Glucose (μmol/mL)	10.7 ± 4.5 (13.7 ± 9.6)	28.1 ± 4.8 (11.8 ± 13.2)	<0.0001 (COV, NS)
FFA (nmol/mL)	985 ± 396 (23.2 ± 12.8)	2,530 ± 955 (42.6 ± 17.2)	<0.0005 (COV, <0.005)
RR (bpm)	37.5 ± 7.4 (12.3 ± 6.1)	49.4 ± 12.7 (14.8 ± 13.3)	<0.05 (COV, NS)
HR (bpm)	261 ± 20 (11.8 ± 8.0)	260 ± 22 (12.7 ± 7.9)	NS (COV, NS)
MBF (mL/g/min)	4.75 ± 2.11	3.53 ± 1.16	NS
MVO_2 (μmol/g/min)	53.3 ± 22.0	36.9 ± 12.7	0.06

COV (%) = variability during PET study; NS = not significant; HbA_{1c} = hemoglobin A_{1c}; FFA = free fatty acids; RR = respiration rate; HR = heart rate; MBF = myocardial blood flow; MVO_2 = myocardial oxygen consumption.

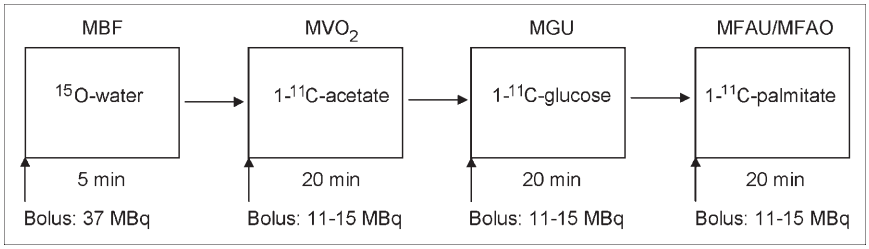

FIGURE 1. PET protocol for GAP studies. Blood sampling was performed throughout the study to determine substrate/insulin plasma levels (6 samples, 5–25 μL) and labeled blood metabolites (15 samples, 5 μL; ^{11}C-CO_2 for 1-^{11}C-acetate and 1-^{11}C-palmitate and ^{11}C-CO_2/^{11}C-lactate for 1-^{11}C-glucose). MBF = myocardial blood flow; MVO_2 = myocardial oxygen consumption; MGU = myocardial glucose utilization; MFAU = myocardial fatty acid utilization; MFAO = myocardial fatty acid oxidation; MFAO/MFAU = myocardial FFA that is oxidized.

injection to measure the contribution of key ^{11}C-metabolites to the total blood radioactive counts ($^{11}CO_2$, %) for 1-^{11}C-acetate and 1-^{11}C-palmitate and total acidic metabolites (TAM, %) for 1-^{11}C-glucose). TAM ($^{11}CO_2$ and ^{11}C-lactate) were separated from neutral and basic species using resin columns as previously reported (*22*). The total ^{11}C-blood activity in each blood sample was measured before being placed on the resin column and was used in conjunction with factor analysis (FA) blood input function measurements.

Kinetic Modeling

Myocardial perfusion and metabolism were measured using compartmental models describing the kinetics of ^{15}O-water (*9,23*), 1-^{11}C-glucose (*7,11*), 1-^{11}C-acetate (*10*), and 1-^{11}C-palmitate (*8*). These models have been extensively validated in large-animal studies and are currently being used in our institution to assess intermediary metabolism in clinical research studies (*12–16*). The validity of using ^{15}O-water for determining myocardial blood flow (MBF) in the rat heart has been shown by comparison with radioactive microspheres (*24*).

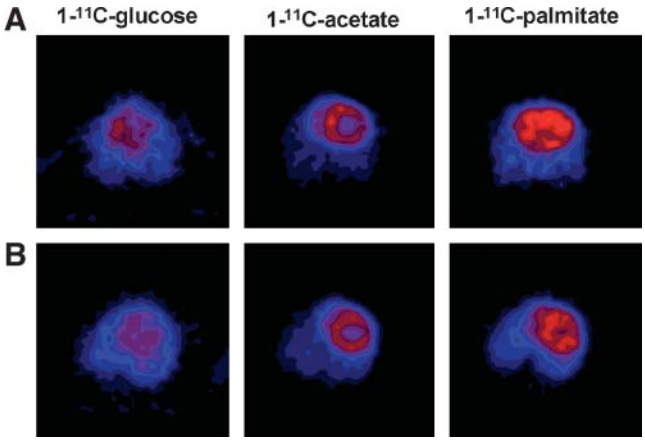

FIGURE 2. Myocardial PET images from a ZDF rat (A) and its lean mate (B) undergoing a GAP study. Images generated by summing data acquired from 0 to 2 min after tracer injection and representing primarily myocardial tracer uptake are shown in transaxial short-axis view. When compared with images from lean control rat, higher glucose and free fatty acid (FFA) accumulation observed in ZDF rat is indicative of higher glucose (1,607 vs. 2,256 nmol/g/min) and FFA utilization (429 vs. 1,394 nmol/g/min). Within the first 2 min after tracer injection, blood 1-^{11}C-acetate time–activity curve showed faster clearance than blood 1-^{11}C-palmitate time–activity curve, resulting in a sharper myocardial 1-^{11}C-acetate image.

To define the kinetics of each tracer, blood (input function) and myocardial tracer activity over time (time–activity curve, counts/pixel/min) were extracted from myocardial sequential PET images using FA methods (*25,26*), which have been previously validated for use in rats (*27*). For a given study, the same 4 or 5 blood and myocardial midventricular transaxial slices were selected manually for each tracer and added to create a 3-dimensional (3D) volume to obtain 3 "pure" factors: right ventricle, left ventricle and myocardium. Because the animals remained under anesthesia for the entire GAP study, it was assumed that the 3D volume generated encompassed the same anatomic volume in all 4 tracers. Two factors, the left ventricular (input function) and myocardial time–activity curves, were then used in conjunction with the appropriate compartmental kinetic models to obtain measurements of perfusion, overall oxidation, and intermediary substrate metabolism for each animal. Because only one global myocardial time–activity curve was generated per tracer, only global—not regional—measurements were obtained.

The number of compartments that are needed to quantify the fate of the tracer in myocardium is directly proportional to the number of steps in the metabolic process being investigated. Compartments are usually represented by boxes or circles and are linked together by arrows representing possible pathways the tracer can follow in a particular metabolic pathway (Fig. 3). Each compartment in a kinetic model is defined as the space in which the tracer is uniformly distributed. The symbol k above or beside each arrow in Figure 3 represents tracer transfer rate constant and denotes the fraction of the total tracer that leaves the compartment per unit time (min^{-1}). The 2 key assumptions of compartmental modeling—tracer is homogeneously distributed in each compartment and the rate of tracer transfer from compartment 1 to compartment 2 is directly proportional to the tracer concentration in compartment 1—make it possible to describe the system under study by *n* first-order, linear differential equations. Each differential equation represents the rate of change of tracer concentration over time in compartment *n*. The solution to the system of differential equations gives the concentration of tracer in each compartment over time (q_n, g/mL). The sum of the concentrations from all compartments (a function of the tracer's blood activity and the turnover rates) represents the myocardial activity over the scanning period (theoretic myocardial time–activity curve). Using numeric nonlinear least-square approaches, turnover rates (k values) can then be estimated by minimizing the differences between the theoretic myocardial time–activity curve predicted by the model and the myocardial time–activity curve obtained from FA of PET images.

In characterizing myocardial perfusion, MBF (mL/g/min) was calculated from ^{15}O-water kinetics (*9,23,28,29*). This modeling approach allows for noninvasive estimation of MBF as well as

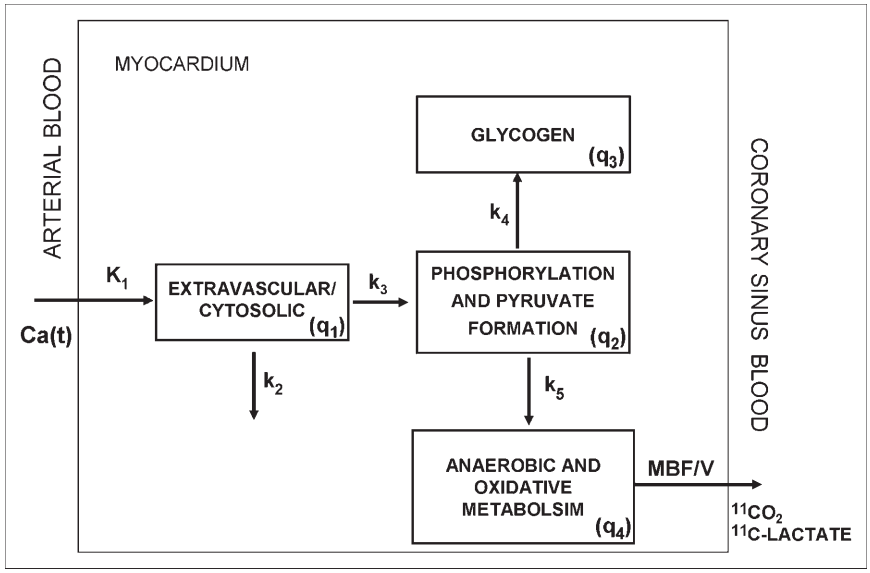

FIGURE 3. Compartmental model representing myocardial 1-^{11}C-glucose kinetics. Ca(t) = blood 1-^{11}C-glucose activity over time (input function, cpm/mL); K_1 (mL/g/min) and k_2–k_5 (min^{-1}) = transfer rate constants; q_n (cpm/mL) = concentration of tracer in compartment *n*; MBF (mL/g/min) = MBF measured from kinetics of ^{15}O-water; V (mL/g) = myocardial fractional vascular volume (assumed to be 10% of total myocardial volume).

PET resolution correction factors (*9,24*): the tissue recovery coefficient (F_{MM}), which is defined as the fraction of true tracer activity observed in the myocardium, and the blood-to-tissue spillover fraction (F_{BM}), which is defined as the fraction of activity originating in the blood pool that is observed in the myocardium. The unique advantages of this approach is that no a priori knowledge of cardiac dimensions is required and that, because these correction fractions are estimated along with the kinetics obtained from a moving heart, they incorporate the smearing effects of cardiac and respiratory motion. For each animal, MBF, F_{MM}, and F_{BM} were estimated from the kinetics of ^{15}O-water after assuming that the left ventricular time–activity curve obtained from FA was the true input function free of partial-volume and spillover effects and that the corresponding myocardial time–activity curve might not be 100% free of these resolution effects. This approach has been validated in normal rats using small-animal PET (*24*). In subsequent metabolic modeling, F_{MM} was fixed to values obtained from the ^{15}O-water kinetics ($F_{MM\text{-}w}$) and F_{BM} was estimated along with the rest of the kinetic parameters. This approach to correct for F_{MM} and F_{BM} has been previously used successfully in the validation of 1-^{11}C-glucose (*7,11*) (Fig. 3) and 1-^{11}C-palmitate (*8*) compartmental models.

Oxygen consumption (MVO_2, μmol/g/min) was estimated from the modeling transfer rate representing 1-^{11}C-acetate oxidation (clearance rate). For the metabolic studies (1-^{11}C-glucose and 1-^{11}C-palmitate), the estimated transfer rates obtained from kinetic modeling were first used to calculate myocardial extraction of tracer (for both 1-^{11}C-glucose [MGEF] and 1-^{11}C-palmitate [MFAEF]) and fractional oxidation [EF-O] and esterification [EF-S] (for 1-^{11}C-palmitate). Myocardial glucose uptake and utilization (MGUP, MGU) and myocardial fatty acid uptake and utilization (MFAUP, MFAU), as well as myocardial fatty acid oxidation (MFAO) and esterification (MFAE) (*16*), respectively, were calculated as follows:

$$^{11}\text{C-tracer uptake}\,(\text{mL/g/min}) = \text{MBF} \times (\text{EF})_{^{11}\text{C-tracer}} \qquad \text{Eq. 1}$$

where MBF estimated from ^{15}O-water kinetics and tracer indicates either glucose or palmitate and EF is the fraction of tracer extracted by the heart and estimated from the kinetics of the tracer using kinetic modeling. Substrate use is defined as:

$$\text{Utilization}\,(\text{nmol/g/min}) = {}^{11}\text{C-tracer uptake} \times [\text{Substrate}]\text{plasma}, \qquad \text{Eq. 2}$$

where [Substrate]plasma is the concentration of glucose or FFA in plasma (nmol/mL).

Similarly, MFAO and MFAE were also calculated from the kinetics of 1-^{11}C-palmitate as follows:

$$\text{MFAO}\,(\text{nmol/g/min}) = [\text{FFA}]\text{plasma} \cdot \text{MBF} \cdot (\text{EF-O}), \qquad \text{Eq. 3}$$

and

$$\text{MFAE}\,(\text{nmol/g/min}) = [\text{FFA}]\text{plasma} \cdot \text{MBF} \cdot (\text{EF-E}), \qquad \text{Eq. 4}$$

where EF-O and EF-E are estimated from the kinetics of 1-^{11}C-palmitate and represent the fraction of extracted 1-^{11}C-palmitate that is rapidly turned over and it is assumed to be oxidized (EF-O) and the fraction that remains in a slow turnover pool and it is assumed to be esterified (EF-F). (i.e., EF = EF-O + EF-E.)

One of the unique features of the noninvasive PET methodology used to assess myocardial substrate (FFA or glucose) utilization lays in its ability to differentiate peripheral from myocardial changes in cardiac substrate utilization. Measurements of total myocardial substrate utilization (nmol/g/min) (Eq. 2), as measured by PET, is the product of myocardial substrate uptake (mL/g/min) (derived from kinetic modeling, Eq. 1) and blood substrate levels (measured from blood samples). Thus, changes in substrate utilization can be due to substrate changes in blood (peripheral effect) or changes in myocardial substrate uptake (myocardial effect).

Statistical Analysis

Mean differences in perfusion and metabolic measurements between ZDF rats and their lean controls were determined by the Student *t* test. *P* values < 0.05 were considered statistically

significant. All group values are presented as mean ± SD. The coefficient of variation during the GAP study (COV, %) for hemoglobin A_{1c} (HbA_{1c}), insulin, glucose, FFA, respiration rate, and heart rate was defined as 100·SD/mean.

RESULTS

The animals' characteristics, plasma substrate levels, and hemodynamics of the ZDF and their littermates used in the GAP PET studies are shown in Table 1. The animals were compared against age-identical littermates and the anticipated changes in HbA_{1c} values as well as plasma substrates (insulin, glucose, and FFAs) were consistent with a type 2 diabetic phenotype. The HbA_{1c} values were more than double in the ZDF rats, with an ≥2-fold elevation in plasma insulin, glucose, and FFA levels compared with lean animals. The variability of plasma insulin and glucose (COV in Table 1) during the study period were comparable for both groups. In contrast, the FFA COV was significantly higher in the ZDF group (COV in Table 1). Although there were no differences in heart rate between ZDF and lean animals and MBF, the respiration rate (RR) was significantly higher and the MVO_2 tended to be significantly lower in the ZDF group. The high RR observed in the ZDF rats was most probably due their susceptibility to acidosis resulting from the reinhalation of expelled CO_2 from the cone piece placed in the animal's snout during the study. An example of microPET images obtained from the 3 metabolic tracers is shown in Figure 2. The quality of the images was similar between the hearts of the lean and the ZDF rats.

F_{MM} and F_{BM} values estimated from ^{15}O-water kinetics were not significantly different between ZDF and Lean ($F_{MM\text{-}w}$, 0.76 ± 0.20 vs. 0.72 ± 0.19, and $F_{BM\text{-}w}$, 0.27 ± 0.14 vs. 0.27 ± 0.15) rats. There were no differences in F_{BM} values between ZDF and lean rats obtained from 1-^{11}C-acetate kinetics ($F_{BM\text{-}ac}$, 0.17 ± 0.11 vs. 0.12 ± 0.11; P = not significant [NS]), 1-^{11}C-palmitate kinetics ($F_{BM\text{-}pal}$, 0.29 ± 0.24 vs. 0.20 ± 0.16; P = NS), or 1-^{11}C-glucose kinetics ($F_{BM\text{-}glu}$, 0.30 ± 0.28 vs. 0.31 ± 0.23; P = NS).

The results obtained in the lean and ZDF rats for myocardial glucose and FFA metabolism are shown in Figures 4 and 5, respectively. In spite of the ZDF group having 2-fold higher levels of insulin than their controls (Table 1), MGUP was not significantly different between the 2 groups (Lean, 0.044 ± 0.041, vs. ZDF, 0.068 ± 0.051 mL/g/min; P = NS). However, because of high levels of plasma glucose in the ZDF group (Lean, 10.7 ± 4.4, vs. ZDF, 28.1 ± 4.9 μmol/mL; $P < 0.0001$) (Fig. 4), MGU tended to be higher in the ZDF group (Lean, 629 ± 785, vs. ZDF, 1,737 ± 1,406 nmol/g/min; $P = 0.06$). During the 1-^{11}C-palmitate study, though MFAUP was not significantly different between the 2 groups (Lean, 0.51 ± 0.28, vs. ZDF, 0.72 ± 0.19 mL/g/min), plasma FFA levels were significantly higher in the ZDF animals when compared with their lean littermates (Lean, 1,052 ± 497, vs. ZDF, 2,277 ± 789 nmol/mL; $P < 0.0005$), resulting in a 3-fold higher MFAU in the ZDF group (Lean, 520 ± 462, vs. ZDF, 1,623 ± 712 nmol/g/min; $P < 0.001$). Consistent with higher MFAU, the ZDF rats showed higher levels of MFAO when compared with their controls (Lean, 453 ± 478, vs. ZDF, 1,363 ± 730 nmol/g/min; $P < 0.01$). No significant differences were observed between groups in the fraction of MFAU that was oxidized most probably due to the large variability of the measurement observed in the lean group (% of MFAO/MFAU: Lean, 79 ± 29, vs. ZDF, 91 ± 4; P = NS) (Fig. 5).

DISCUSSION

The ability to quantify myocardial metabolic changes in rats provides a valuable tool to the researcher in the design and implementation of new diagnostic and treatment strategies. Small-animal PET, a recent development in the imaging arsenal, offers the possibility of undertaking noninvasive longitudinal imaging, examining in detail the myocardial phenotype (*4–6*). There are, however, challenges presented to the imaging scientist with regard to the ability to accurately quantify metabolic data in a rat myocardium. Issues with regard to partial-volume, motion, and spillover effects may seriously hinder the ability of the imaging scientist to quantify PET data in the rat myocardium. We undertook this study to establish methodology to

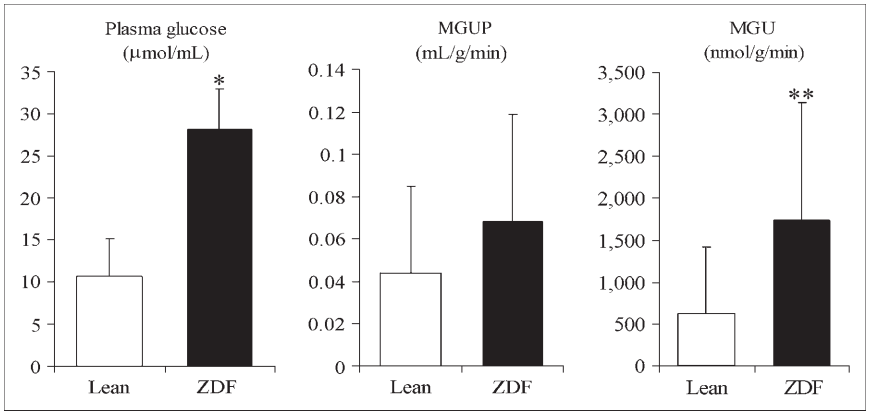

FIGURE 4. Glucose metabolism measurements obtained in ZDF and lean rats by compartmental modeling of 1-^{11}C-glucose PET data. MGUP = myocardial glucose uptake; MGU = myocardial glucose utilization. *$P < 0.0001$; **$P = 0.06$ (■, ZDF; □, Lean).

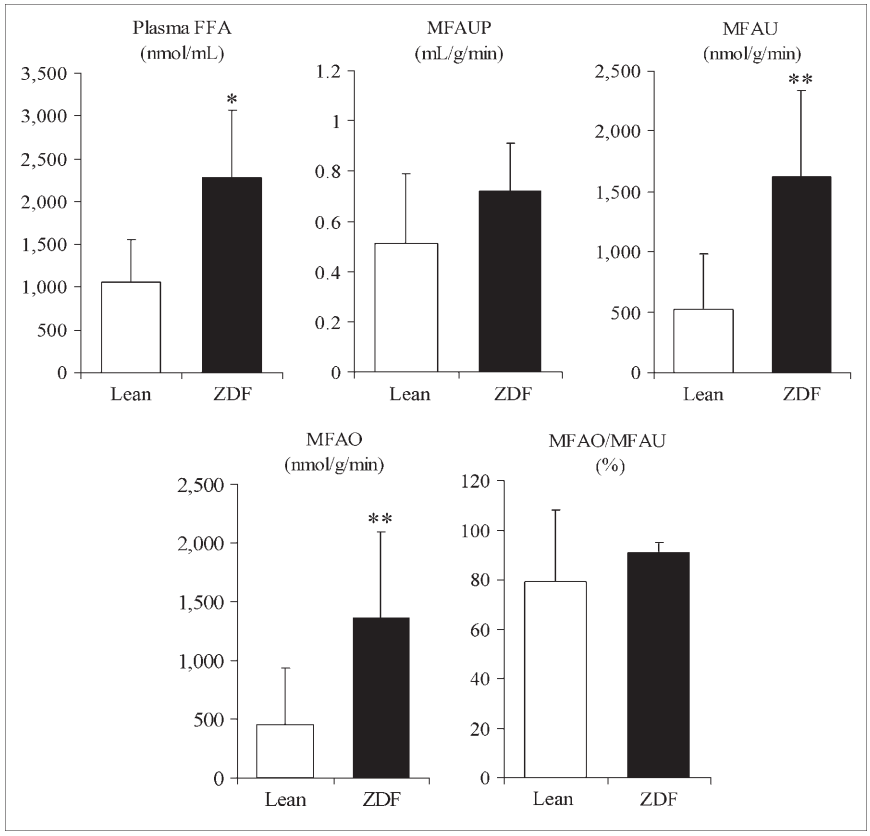

FIGURE 5. FFA metabolism measurements obtained in ZDF and lean rats by compartmental modeling of 1-^{11}C-palmitate PET data. MFAUP = myocardial fatty acid uptake; MFAU = myocardial fatty acid utilization; MFAO = myocardial fatty acid oxidation; MFAO/MFAU = myocardial FFA that was oxidized. *$P < 0.001$; **$P < 0.01$ (■, ZDF; □, Lean).

enable the quantification of myocardial substrate metabolism in rats. We used a well-characterized rat model of diabetes mellitus in conjunction with small-animal PET and well-defined kinetic models to demonstrate the proof of concept. We demonstrate in this study that, by using this approach, it is feasible to accurately and noninvasively delineate metabolic changes in the rat myocardium.

Because of the small size of the rat heart we were unable to perform conventional arteriovenous balance studies that are typically used to verify the accuracy of new PET radiotracer techniques in studies of large animals or humans (*8,11,30*). Acute tissue autoradiographic methods could have been used to evaluate the absolute retention of radiotracer in rat heart. However, this method does not provide the necessary temporal information to permit the comparison with our PET kinetic models. Consequently, we performed this proof-of-concept study by using the ZDF rat model, which faithfully recapitulates many aspects of the human metabolic syndrome (*31*). ZDF rats have been used extensively as a model of type 2 diabetes mellitus, examining the multiple aspects of this disease, including prevention, progression, and complications (*32*). Not only do the majority of young male ZDF rats develop symptoms of the diabetic syndrome—by becoming insulin resistant and later overtly obese—but also they respond well to drugs (e.g., glitazones or metformin) targeted toward the treatment of humans with type 2 diabetes mellitus. ZDF rats also develop a cardiomyopathic phenotype associated with type 2 diabetes mellitus (*33*). Although the cause(s) of this phenotype is unclear, the myopathy is hypothesized to be at least partially the result of the increase in myocardial fatty acid metabolism (*33*). With the advent of noninvasive small-animal PET technologies and the validated use of GAP PET studies to delineate myocardial metabolism in humans, we undertook the current feasibility study to establish the practicality and efficacy of imaging quantitative changes in the myocardial metabolism of ZDF rats as the diabetic syndrome develops.

The ZDF animals were studied within 2 mo from the onset of diabetes; thus, observations of metabolic changes in these animals should be consistent with the metabolic changes that take place during the early stages of type 2 diabetes mellitus. The lean littermates acted as controls against the ZDF animals and demonstrated the anticipated alterations in HbA_{1c}, insulin, glucose, and FFA levels consistent with the advent of type 2 diabetes mellitus in the ZDF rats at the time of study. The results of this feasibility study are consistent with the well-known metabolic changes that take place in the heart of the ZDF rat. Simply stated, when compared with their lean controls, the ZDF rat showed (a) elevated insulin, glucose, and FFA levels; (b) elevated FFA utilization and oxidation; (c) preserved myocardial glucose utilization; and (d) a trend toward a lower MVO_2. The metabolic data obtained noninvasively in this study using small-animal PET and well-established kinetic modeling approaches is consistent with

the well-known early metabolic derangements of the diabetic heart, which include high fatty acid uptake, utilization, and oxidation that precedes glucose metabolism changes (*32,34*). For example, Aasum et al. (*34*), using invasive ex vivo procedures, demonstrated in *db/db* mice that diabetic hearts exhibit increased fatty acid oxidation that preceded reductions in carbohydrate oxidation. Wang et al. (*35*) have shown that the rate·pressure product and coronary flow (mL/g/min) were reduced in 12-wk-old isolated hearts of (not paced) male ZDF rats when compared with their lean controls. Their animals were fed the same chow as in this study (Purina 5008), were similar in age and weight, and were studied under glucose and insulin plasma levels comparable with ours. In a subsequent study in which isolated hearts of 12-wk-old (paced) ZDF rats and their lean controls were studied under conditions to mimic the fed state, Wang et al. (*36*) observed that, at rest, the ZDF rats exhibited higher FFA oxidation and lower lactate, and, to a lesser extent, pyruvate oxidation, with no differences in glucose oxidation and MVO_2. Furthermore, they observed no differences in oxidative ATP production between ZDF and control rats.

Results of studies in isolated perfused hearts (*37*) as well as in vivo (*38*) have shown that the glucose transporter GLUT-4 is downregulated in 8-wk-old (*37*) and 12-wk-old (*38*) ZDF rats, resulting in lower glucose uptake (*38*) and oxidation (*37*) in the ZDF rats when compared with their lean controls. In the present study, when compared with their lean controls, we observed comparable levels of glucose uptake in the ZDF rats in spite of 2-fold higher insulin levels in these animals. Moreover, high glucose blood levels resulted in a strong trend toward higher glucose utilization in the ZDF rats. However, measurements of myocardial substrate metabolism were performed under fasting conditions, which result in FFA being the primary source of cardiac energy. Under these conditions, myocardial glucose extraction and oxidation by the heart is very low. The low extraction of tracer results in myocardial time–activity curves with low counts and high noise and, consequently, potential poor estimates of myocardial glucose extraction. In the present study, in contrast to myocardial uptake of 1-^{11}C-palmitate, which ranged from 0.03 to 0.95 mL/g/min, myocardial uptake of 1-^{11}C-glucose ranged from $<$0.01 to 0.13 mL/g/min. The low extraction of 1-^{11}C-glucose by myocardium most likely contributed to the large group variability observed in glucose uptake in both Lean (93% COV) and ZDF (75% COV) rats (Fig. 3). This variability was much larger than the variability observed in glucose uptake measurements done in lean subjects studied under fed conditions ($n = 11$) and type 1 diabetics studied during an insulin drip ($n = 11$) using the same modeling methodology (lean, 40% COV; type 1 diabetics, 59% COV) (*12*). To overcome this problem, studies designed to assess glucose metabolism could be done under conditions of high myocardial glucose use, such as fed or hyperinsulinemic–euglycemic clamping conditions.

The results of this study are consistent with the well-established early onset of cardiac substrate metabolic derangement in the ZDF rat, demonstrating that noninvasive measurements of cardiac substrate metabolism is feasible in rats using kinetic modeling in conjunction with PET tracers and dynamic microPET imaging. However, there are several issues pertaining to the methodology used that need to be addressed. The use of isoflurane for anesthesia in rodents is the preferred method because of the rapid induction and recovery from anesthesia (*22*). Other anesthetics prevent the possibility of long imaging studies (4 h) and recovery from surgery. Evidence in dogs suggests that, after 10 min of isoflurane, both plasma FFA concentration and palmitate turnover decreased by $>$70% throughout the remainder of the anesthesia (*39*). In the same study, glucose production increased after induction of anesthesia and peripheral glucose utilization decreased after 3.5 h of isoflurane anesthesia. These data, therefore, suggest a widespread and immediate metabolic effect during isoflurane anesthesia. However, careful attention to detail, including the monitoring of FFA levels and data based on comparisons between ZDF and lean littermates, as well as the application of accurately defined kinetic models, takes these factors into account.

All kinetic models are implemented under the assumption that the system under study is in steady state. In the present study, although the variability of FFA during microPET imaging was higher in the ZDF group, heart rate, plasma insulin, and glucose variability during microPET imaging were comparable between the ZDF rats and their controls. However, insulin, glucose, and FFA variability was relatively large (Table 1), partially because of the length of the imaging studies (4–6 h). To minimize these relatively large physiologic variations in insulin and substrate levels, interventions such as euglycemic–hyperinsulinemic clamp or constant infusion of low-dose intralipid might be desirable.

The poor resolution of current microPET scanners ($\sim$2.0-mm full width at half maximum) in relation to the very small dimensions of the rat heart (approximately 2-mm wall thickness and 5.5-mm left ventricular diameter) results in severe distortion of blood and myocardial time–activity curves generated from dynamic cardiac microPET images. Blood (input function) and myocardial time–activity curves—the key data required for kinetic modeling—must be corrected for these resolution effects. In the present study both blood and myocardial time–activity curves for all tracers used were extracted from microPET cardiac images by FA. This approach results in uncontaminated blood time–activity curves and myocardial time–activity curves with relatively low contamination ($F_{MM\text{-}w}$ [$n = 10$] = 0.90 $\pm$ 14; $F_{BM\text{-}all}$ [$n = 40$] = 0.11 $\pm$ 11). However, this approach does not allow for the extraction of regional myocardial curves, because only 1 global blood and 1 global myocardial curve per tracer are generated. Our group is currently implementing new reconstruction

algorithms as well as cardiac gating strategies designed to minimize these resolution effects so that regional analysis of data could be implemented.

Although the results of this feasibility study are consistent with what is known about the myocardial changes in substrate metabolism that occur in the early onset of diabetes, the relatively large variability among animals in substrate and insulin levels (Table 1) as well as myocardial substrate metabolism (Figs. 4 and 5) observed in both lean and ZDF rats is multifactorial. These factors include natural physiologic variability, fluctuations in glucose and FFA metabolism associated with isoflurane anesthesia as well as with the long duration of the studies (4–6 h), and the uncertainties in measurements associated with the complex modeling approaches implemented, such as noise of PET data, estimation (vs. direct measurement) of model parameters and partial-volume and spillover effects, and correction of blood PET data for blood ^{11}C-metabolites. Thus, to optimize these complex studies, by removing or minimizing some of these sources of error, more systematic studies are required. These studies should include sequential studies in the same animal in which substrate and insulin levels are maintained constant during PET data acquisition and the use of different anesthetics is investigated. Once the animal protocol is optimized, uncertainty and variability of the measurements obtained from these modeling approaches could be further evaluated and optimized by continuing to develop methods to improve data obtained from a small-animal PET scanner (by minimizing partial-volume and spillover effects and enhancing signal to noise ratios), such as the implementation of respiratory gating and new reconstruction algorithms.

It is also important to note that the studies presented here have been performed in a rat model of cardiac disease, and translation to the mouse (the most common form of transgenic model) will require an additional stage of validation. The smaller size of the mouse myocardium will exacerbate partial-volume and spillover effects. Spatial resolution and sensitivity may be issues if syndromes such as ischemia are to be examined. We are continuing to develop methods to use with the mouse myocardium, such as the implementation of respiratory gating and new reconstruction algorithms to overcome these potential limitations.

Implementation of the current methodology is challenging as it requires a wide range of expertise and resources, such as animal technologists, radiochemists, physicists, mathematical modelers, and data analysts as well as access to a cyclotron and the ability to produce on demand the radiotracers used. In spite of these challenges, our institution is currently implementing these methods successfully in clinical studies designed to elucidate the potential impact that alterations in cardiac substrate metabolism attributed to different diseases, such as diabetes and cardiomyopathy, have on cardiac function. Nonetheless, the quantification of myocardial perfusion and metabolism in small animals is not limited to the use of the tracers used in the present study. Following the work presented in this article, other tracers to quantify metabolism and other biologic processes in the myocardium and other tissues can be validated in a similar manner.

CONCLUSION

This study demonstrates that noninvasive measurements of myocardial substrate metabolism are feasible in rat models of human diseases using small-animal PET and tracer kinetic modeling. Although further studies are required to optimize the animal protocol and the methodology used in both rats and mice, these quantitative and noninvasive animal PET techniques should prove useful in the translation of observations obtained in rodent models of cardiac disease to humans.

ACKNOWLEDGMENTS

We thank John A. Engelbach, Nicole Fettig, Lori Strong, Margaret M. Morris, and Jerrel Rutlin for technical assistance. We also thank Kooresh Shoghi, PhD, for helpful discussions. This work was supported by NIH/NHLBI grant 2-PO1-HL-13851.

REFERENCES

1. Lewis JS, Achilefu S, Garbow JR, Laforest R, Welch MJ. Small animal imaging: current technology and perspectives for oncological imaging. *Eur J Cancer.* 2002;38:2173–2188.
2. Finck BN, Lehman JJ, Leone TC, et al. The cardiac phenotype induced by PPARα overexpression mimics that caused by diabetes mellitus. *J Clin Invest.* 2002;109:121–130.
3. Aasum E, Belke DD, Severson DL, et al. Cardiac function and metabolism in type 2 diabetic mice after treatment with BM 17.0744, a novel PPAR-alpha activator. *Am J Physiol Heart Circ Physiol.* 2002;283:H949–H957.
4. Bentourkia M, Croteau E, Langlois R, et al. Cardiac studies in rats with ^{11}C-acetate and PET: a comparison with ^{13}N-ammonia. *IEEE Trans Nucl Sci.* 2002; 49:2322–2327.
5. Lecomte R, Croteau E, Gauthier ME, et al. Cardiac PET imaging of blood flow, metabolism, and function in normal and infarcted rats. *IEEE Trans Nucl Sci.* 2004;51:696–704.
6. Kudo T, Fukuchi K, Annala AJ, et al. Noninvasive measurement of myocardial activity concentrations and perfusion defect sizes in rats with a new small-animal positron emission tomograph. *Circulation.* 2002;106:118–123.
7. Herrero P, Sharp TL, Dence C, Haraden BM, Gropler RJ. Comparison of 1-^{11}C-glucose and ^{18}F-FDG for quantifying myocardial glucose use with PET. *J Nucl Med.* 2002;43:1530–1541.
8. Bergmann SR, Weinheimer CJ, Markham J, Herrero P. Quantitation of myocardial fatty acid metabolism using PET. *J Nucl Med.* 1996;37:1723–1730.
9. Bergmann SR, Herrero P, Markham J, Weinheimer CJ, Walsh MN. Noninvasive quantitation of myocardial blood flow in human subjects with oxygen-15-labeled water and positron emission tomography. *J Am Coll Cardiol.* 1989;14:639–652.
10. Beanlands RS, Bach DS, Raylman R, et al. Acute effects of dobutamine on myocardial oxygen consumption and cardiac efficiency measured using carbon-11 acetate kinetics in patients with dilated cardiomyopathy. *J Am Coll Cardiol.* 1993;22:1389–1398.
11. Herrero P, Weinheimer CJ, Dence C, Oellerich W, Gropler RJ. Quantification of myocardial glucose utilization by PET and 1-carbon-11-glucose. *J Nucl Cardiol.* 2002;9:5–14.
12. Herrero P, Peterson LR, McGill JB, et al. Increased myocardial fatty acid metabolism in patients with type 1 diabetes mellitus. *J Am Coll Cardiol.* 2006;47:598–604.
13. Davila-Roman VG, Vedala G, Herrero P, et al. Altered myocardial fatty acid and glucose metabolism in idiopathic dilated cardiomyopathy. *J Am Coll Cardiol.* 2002;40:271–277.
14. Kates AM, Herrero P, Dence C, et al. Impact of aging on substrate metabolism by the human heart. *J Am Coll Cardiol.* 2003;41:293–299.

15. Peterson LR, Eyster D, Davila-Roman VG, et al. Short-term oral estrogen replacement therapy does not augment endothelium-independent myocardial perfusion in postmenopausal women. *Am Heart J.* 2001;142:641–647.
16. Dence CS, Herrero P, Schwarz SW, Mach RH, Gropler RJ, Welch MJ. Imaging myocardium enzymatic pathways with carbon-11 radiotracers. *Methods Enzymol.* 2004;385:286–315.
17. Welch MJ, Kilbourn MR. A remote system for the routine production of oxygen-15 radiopharmaceuticals. *J Labelled Compds Radiopharm.* 1985;22:1193–1200.
18. Dence CS, Powers WJ, Gropler RJ, Welch MJ. High yield synthesis of 1-[^{11}C]glucose for clinical applications: problems and solutions. *J Labelled Compds Radiopharm.* 1997:777–778.
19. Welch MJ, Wittmer SL, Dence CS, Tewson TJ. Radiopharmaceuticals labeled with ^{11}C and ^{18}F: considerations related to the preparation of ^{11}C-palmitate. In: Root JW, Krohn KA, eds. *Short-Lived Radionuclides in Chemistry and Biology.* Vol. 197. Washington, DC: American Chemistry Society Advances in Chemistry Series; 1981:407–417.
20. Knoess C, Siegel S, Smith A, et al. Performance evaluation of the microPET R4 PET scanner for rodents. *Eur J Nucl Med Mol Imaging.* 2003;30:737–747.
21. Tai YC, Ruangma A, Rowland DJ, et al. Performance evaluation of the microPET Focus: a third-generation microPET scanner dedicated to animal imaging. *J Nucl Med.* 2005;46:455–463.
22. Sharp TL, Dence CS, Engelbach JA, Herrero P, Gropler RJ, Welch MJ. Advances in techniques necessary for multi-parametric small animal imaging studies. *Nucl Med Biol.* 2005;32:875–884.
23. Herrero P, Hartman JJ, Senneff MJ, Bergmann SR. Effects of time discrepancies between input and myocardial time-activity curves on estimates of regional myocardial perfusion with PET. *J Nucl Med.* 1994;35:558–566.
24. Herrero P, Kim J, Sharp TL, et al. Assessment of myocardial blood flow using ^{15}O-water and 1-^{11}C-acetate in rats with small-animal PET. *J Nucl Med.* 2006; 47:477–485.
25. Di Paola R, Bazin JP, Aubry F. Handling of dynamic sequences in nuclear medicine. *IEEE Trans Nucl Sci.* 1982;NS29:1310–1321.
26. Wu HM, Hoh CK, Choi Y, et al. Factor-analysis for extraction of blood time-activity curves in dynamic FDG-PET studies. *J Nucl Med.* 1995;36: 1714–1722.
27. Kim J, Herrero P, Sharp TL, et al. A minimally invasive method of determining blood input function from PET images in rodents. *J Nucl Med.* 2006;47:330–336.
28. Herrero P, Staudenherz A, Walsh JF, Gropler RJ, Bergmann SR. Heterogeneity of myocardial perfusion provides the physiological basis of perfusable tissue index. *J Nucl Med.* 1995;36:320–327.
29. Herrero P, Markham J, Bergmann SR. Quantitation of myocardial blood flow with $H_2{}^{15}O$ and positron emission tomography: assessment and error analysis of a mathematical approach. *J Comput Assist Tomogr.* 1989;13:862–873.
30. Sun KT, Yeatman LA, Buxton DB, et al. Simultaneous measurement of myocardial oxygen consumption and blood flow using [1-carbon-11]acetate. *J Nucl Med.* 1998;39:272–280.
31. Bray GA. The Zucker-fatty rat: a review. *Fed Proc.* 1977;36:148–153.
32. Unger RH, Orci L. Diseases of liporegulation: new perspective on obesity and related disorders. *FASEB J.* 2001;15:312–321.
33. Zhou YT, Grayburn P, Karim A, et al. Lipotoxic heart disease in obese rats: implications for human obesity. *Proc Natl Acad Sci U S A.* 2000;97: 1784–1789.
34. Aasum E, Hafstad AD, Severson DL, Larsen TS. Age-dependent changes in metabolism, contractile function, and ischemic sensitivity in hearts from db/db mice. *Diabetes.* 2003;52:434–441.
35. Wang P, Chatham JC. Onset of diabetes in Zucker diabetic fatty (ZDF) rats leads to improved recovery of function after ischemia in the isolated perfused heart. *Am J Physiol Endocinol Metab.* 2004;286:E725–E736.
36. Wang P, Lloyd SG, Zeng H, Bonen A, Chatham JC. Impact of altered substrate utilization on cardiac function in isolated hearts from Zucker diabetic fatty rats. *Am J Physiol Heart Circ Physiol.* 2004;288:H2102–H2110.
37. Golfman LS, Wilson CR, Sharma S, et al. Activation of PPAR enhances myocardial glucose oxidation and improves contractile function in isolated working hearts of ZDF rats. *Am J Physiol Endocrinol Metab.* 2005;289:E328–E336.
38. Pelzer T, Jazbutyte V, Arias-Loza PA, et al. Pioglitazone reverses down-regulation of cardiac PPAR expression in Zucker diabetic fatty rats. *Biochem Biophys Res Commun.* 2005;329:726–732.
39. Horber FF, Krayer S, Miles J, Cryer P, Rehder K, Haymond MW. Isoflurane and whole body leucine, glucose, and fatty acid metabolism in dogs. *Anesthesiology.* 1990;73:82–92.